Screened Coulomb Interactions With Non-uniform Surface Charge

Sandip Ghosal
Department of Mechanical Engineering
& Engineering Sciences and Applied Mathematics,
Northwestern University, Evanston, IL 60208, USA

John D. Sherwood
Department of Applied Mathematics and Theoretical Physics,
University of Cambridge, Cambridge CB3 0WA, UK

February 16, 2017

Abstract

The screened Coulomb interaction between a pair of infinite parallel planes with spatially varying surface charge is considered in the limit of small electrical potentials for arbitrary Debye lengths. A simple expression for the disjoining pressure is derived in terms of a two dimensional integral in Fourier space. The integral is evaluated for periodic and random charge distributions and the disjoining pressure is expressed as a sum over Fourier-Bloch reciprocal lattice vectors or in terms of an integral involving the autocorrelation function respectively. The force between planes with a finite area of uniform charge, a model for the DLVO interaction between finite surfaces, is also calculated. It is shown that the overspill of the charge cloud beyond the region immediately between the charged areas results in a reduction of the disjoining pressure, as reported by us recently in the long Debye length limit for planes of finite width.

1 Introduction

The force of interaction between neighboring dielectric-electrolyte interfaces is responsible for a wide range of phenomena such as the stability of colloidal suspensions [1], colloidal self-assembly [2], and the stability of thin liquid films [3]. The nature of the interaction is generally a short range ($\sim$ 1 nm) attraction due to molecular van der Waals forces and a longer range ($\sim$ 100 nm) electrostatic repulsion that is partially screened by the free ions in the electrolyte. Analysis of the force between particles was provided by Derjaguin & Landau [4] and by Verwey and Overbeek [5]. The expression for the force or the interaction potential that they derived and the theory of colloid stability based on it has become the

bedrock of most investigations of the subject and is referred to as "DLVO theory". The original DLVO approximation has been improved and extended [6–10] over the years. When DLVO theory was developed, it could only be tested by comparing its predictions against experimental observations of large scale phenomena such as the onset of flocculation in colloidal systems. This changed with the introduction of the surface force apparatus capable of measuring pico-Newton interaction forces between atomically smooth mica surfaces [11–15]. More recently, other precision instruments such as atomic force microscopes [16] and laser optical tweezers [17, 18] have been used to measure directly these small scale interfacial forces. These experiments have generally confirmed the theory within its expected range of validity. However, uncertainties in the interpretation of these experiments remain for separations smaller than a few nanometers, in the regime where the interaction changes from repulsive to attractive [19, 20] due to the molecular van der Waals forces.

In addition to new and distinct mechanisms [20] that have been discussed to explain the interaction at short distances, the details of the screened Coulomb interaction model itself are important. For example, at such small separations, the predictions of the constant charge, constant potential and charge regulation models yield distinctly different results [1, 20–23]. Furthermore, in this regime, it is impossible to invoke the simplifying assumption that there is only a slight overlap of the Debye layers adjacent to the two surfaces. If the lateral extent of the interacting surfaces is also small (as in nanocolloids, tips of atomic force microscopes or clay particles) then overspill of the Debye layer out of the region immediately between the surfaces can become important [24]. Recent variants of the classical surface force experiment have shown significant anomalies that have not yet been fully explained: surfactant coated mica surfaces show a long range attraction [25–27] in place of the expected repulsion. It has been suggested [27] that this could be due to a patchy distribution of the surfactant on the mica surface which creates alternate domains of positive and negative surface charges that are able to dynamically self-adjust as the surfaces approach each other. A small scale feature of all charged interfaces is that the charge resides at discrete locations on the surface. While it seems appropriate to ignore this feature at distances large compared to the scale of this granularity, such an assumption may not be valid when considering the interactions at very short range. The effect of this granularity in charge distribution has been the focus of a number of studies [28–31].

In this paper we examine the general problem of the interaction of a pair of infinite parallel planes, each with an arbitrary prescribed distribution of surface charge. The space between the planes is filled with an electrolyte. We derive an expression for the normal force acting on either surface by integrating the Maxwell stress over the central plane midway between the two surfaces. We follow Richmond [32] in our use of Fourier transform techniques, but our approach provides a more direct route to the final result than previous investigations based on calculating the free energy of the system [28, 30–34]. In particular, we consider the problem of a uniformly charged central section and calculate the effect of charge overspill on the disjoining pressure. The model of infinite planes that we adopt here (Figure 1) allows us to derive analytical results for arbitrary Debye length,

whereas in earlier work [24] the disjoining pressure between finite blocks was found only in the limit of long Debye length. We shall also show how our expression for the interaction force can be used to determine the disjoining pressure in other cases, such as periodic or random distributions of charges.

The paper is organized as follows. In the next section we define our problem and show that the case of an arbitrary charge distribution may be analyzed within the framework of the linearized Poisson-Boltzmann equation by considering separately the situations where the charge distributions on the two planes are identical (the symmetric case) and where the charge distribution is identical but with opposite sign (the antisymmetric case). In section 3 the solution for the potential is obtained in terms of Fourier transforms with respect to co-ordinates with axes parallel to the planes. In section 4 we develop an expression for the normal interaction force in terms of an integral of the Maxwell stress over the central plane midway between the charged surfaces. In section 5 we evaluate the integral to determine the disjoining pressure for finite charged patches, periodic distributions of charge and random charge distribution. In section 6 we discuss the range of validity of our methods, and conclusions are given in section 7.

2 Formulation

Consider an electrolyte filled gap of uniform width $(2h)$ within a dielectric solid. The electrolyte contains N charged species of valence z_i, $i = 1, \ldots, N$, with $n_i^{(\infty)}$ the equilibrium number density of the i th species far from any charged surfaces. The charge distributions on the confining walls located at $z = h$ and $z = -h$ are respectively $\sigma_+(x, y)$ and $\sigma_-(x, y)$. The geometry is as shown in Figure 1 (left panel). We wish to calculate the component of the force orthogonal to the walls (in the z direction) on the plane at $z = h$. Clearly, the normal force on the other plane is equal and opposite. The problem is treated in the Debye-Hückel limit [1], in which all potentials are assumed small compared to the thermal scale k_BT/e, where e is the magnitude of the electron charge and k_BT the Boltzmann temperature. The solid substrate surrounding the channel is assumed to have permittivity $\epsilon_s = 0$. This approximation is commonly invoked since the relative permittivity of water ($\sim$ 80) is much larger than that of most nonpolar solid substrates ($\sim$ 2 – 4). In this section, we assume that charge distributions are sufficiently localized so that the functions σ_+^2, σ_-^2 and $\sigma_+\sigma_-$ are all integrable over the (x, y) plane. This restriction is relaxed in section 5 where we consider periodic and random distributions. In the Debye-Hückel limit, the equilibrium potential ϕ satisfies the linearized Poisson-Boltzmann equation

$$\nabla^2\phi = \kappa^2\phi, \tag{1}$$

where κ^{-1} is the Debye length.

We define the symmetric case as that in which both planes have the charge distribution $\sigma_S(x, y)$. In the antisymmetric case, the charge density is $\sigma_A(x, y)$ on $z = h$ and $-\sigma_A(x, y)$

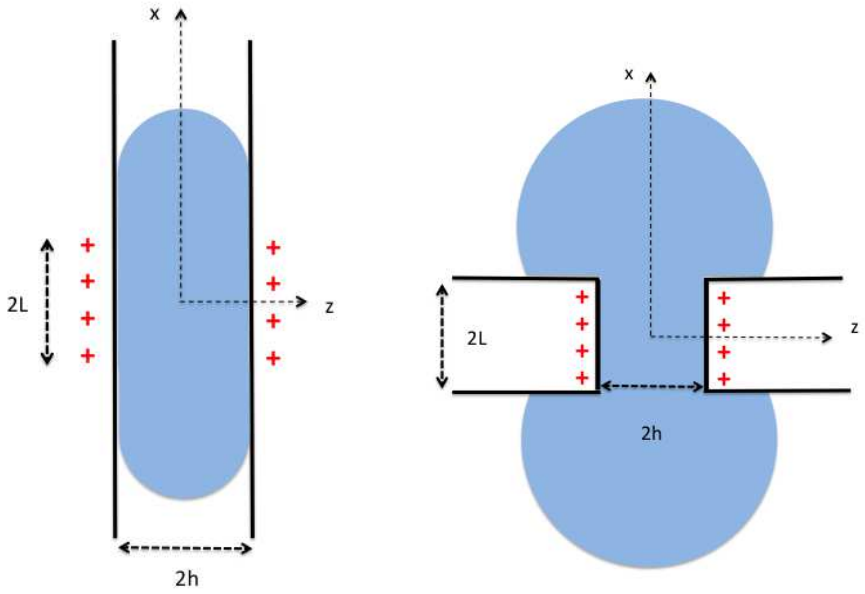

Figure 1: Sketch showing the geometry of the confined problem (left) and the unconfined problem (right).

on $z = -h$. Thus, the potentials $\phi = \phi_S$ and $\phi = \phi_A$ for the symmetric and antisymmetric problems respectively, satisfy (1) and the boundary conditions

$$\partial_z \phi_S(x, y, \pm h) = \pm \sigma_S(x, y)/\epsilon, \qquad \partial_z \phi_A(x, y, \pm h) = \sigma_A(x, y)/\epsilon, \tag{2}$$

where ϵ is the electrolyte permittivity. For arbitrary charge distributions $\sigma_+(x, y)$ on $z = h$ and $\sigma_-(x, y)$ on $z = -h$ we construct the corresponding symmetric and antisymmetric charge distributions

$$\sigma_S = \frac{1}{2}(\sigma_+ + \sigma_-), \qquad \sigma_A = \frac{1}{2}(\sigma_+ - \sigma_-). \tag{3}$$

Then, the equilibrium potential is $\phi(x, y, z) = \phi_S(x, y, z) + \phi_A(x, y, z)$. Indeed, ϕ clearly satisfies (1) since ϕ_S and ϕ_A do, and also satisfies the boundary conditions:

$$\epsilon \partial_z \phi(x, y, \pm h) = \pm \sigma_S + \sigma_A = \begin{cases} \sigma_+ & \text{if } z = +h, \\ -\sigma_- & \text{if } z = -h. \end{cases} \tag{4}$$

3 Solutions in Fourier space

We use a caret $\widehat{\ }$ to indicate Fourier transforms with respect to variables x and y. Thus,

$$\hat{\phi}(k_x, k_y, z) = \frac{1}{(2\pi)^2} \int \phi(x, y, z) \exp[-i(k_x x + k_y y)]\, dxdy, \tag{5}$$

$$\phi(x, y, z) = \int \hat{\phi}(k_x, k_y, z) \exp[i(k_x x + k_y y)]\, dk_x dk_y. \tag{6}$$

Equations (1) and (2) imply that $\hat{\phi}$ satisfies

$$\partial_{zz}\hat{\phi} = (k^2 + \kappa^2)\hat{\phi} \qquad \text{with} \qquad \epsilon\partial_z\hat{\phi}(k_x, k_y, \pm h) = \begin{cases} \pm\hat{\sigma}_S \\ \hat{\sigma}_A \end{cases} \tag{7}$$

where $k^2 = k_x^2 + k_y^2$. The two cases in (7) correspond to the symmetric and anti-symmetric problems respectively. The solution to (7) is readily obtained:

$$\hat{\phi}(k_x, k_y, z) = \begin{cases} \hat{\sigma}_S \cosh(Kz)/[\epsilon K \sinh(Kh)] \\ \hat{\sigma}_A \sinh(Kz)/[\epsilon K \cosh(Kh)] \end{cases} \tag{8}$$

where $K = (\kappa^2 + k^2)^{1/2}$.

4 The normal force

The z-component of the force is given as the integral of the zz component Σ_{zz} of the total stress over the the central plane S ($z = 0$) between the plates [1]

$$F_z = -\int_S \Sigma_{zz}\, dxdy, \qquad \Sigma_{zz} = -\,p_{\rm os}|_{z=0} - \frac{\epsilon}{2}|\boldsymbol{\nabla}_h\phi_0|^2 + \frac{\epsilon}{2}|\phi_0'|^2, \tag{9}$$

where $\phi_0(x, y) = \phi(x, y, 0)$, $\phi_0'(x, y) = (\partial_z\phi)_{z=0}$, $\boldsymbol{\nabla}_h = \hat{\boldsymbol{\imath}}\partial_x + \hat{\boldsymbol{\jmath}}\partial_y$, and

$$p_{\rm os} = k_B T \sum_{i=1}^{N} n_i = k_B T \sum_{i=1}^{N} n_i^{(\infty)} \exp(-ez_i\phi/k_B T) \tag{10}$$

represents the osmotic pressure. We have neglected the uniform background pressure that gives no contribution to the force. Equation (9) is quite general and is applicable even when the potential ϕ is not small compared to the thermal scale, $k_B T/e \approx 25$ mV at room temperature. In the Debye-Hückel limit $\phi \ll k_B T/e$ we have the approximate form

$$p_{\rm os} = k_B T \sum_{i=1}^{N} n_i^{(\infty)} \exp(-ez_i\phi/k_B T) \approx k_B T \sum_{i=1}^{N} n_i^{(\infty)} + \frac{1}{2}\epsilon\kappa^2\phi^2. \tag{11}$$

In the case of a symmetric two component electrolyte $z_1 = -z_2 = z$, $n_1^{(\infty)} = n_2^{(\infty)} = n_\infty$, and thus, $p_{\rm os} = 2n_\infty k_B T \cosh(ez\phi/k_B T)$. In this paper we discuss the case of low potentials where (11) is applicable.

4.1 The symmetric problem

In the symmetric problem, the last term in the expression for Σ_{zz} in (9) vanishes, and hence,

$$F_z = \frac{\epsilon}{2}\int \left(\kappa^2\phi_0^2 + |\boldsymbol{\nabla}_h\phi_0|^2\right)\, dxdy = 2\pi^2\epsilon\int K^2|\hat{\phi}_0|^2\, dk_x dk_y, \tag{12}$$

where the final form follows upon the application of Parseval's identity for Fourier transforms. On substituting the solution (8) to the symmetric problem, we have

$$F_z = \frac{2\pi^2}{\epsilon}\int |\hat{\sigma}_S|^2\,\mathrm{cosech}^2(Kh)\, dk_x dk_y. \tag{13}$$

4.2 The antisymmetric problem

For the antisymmetric problem, $\phi_0(x,y) = 0$ and $\hat{\phi}_0' = \hat{\sigma}_A\,\mathrm{sech}(Kh)/\epsilon$. Therefore,

$$F_z = -2\pi^2\epsilon\int |\hat{\phi}_0'|^2\, dk_x dk_y = -\frac{2\pi^2}{\epsilon}\int |\hat{\sigma}_A|^2\,\mathrm{sech}^2(Kh)\, dk_x dk_y. \tag{14}$$

The force is negative, indicating an attractive interaction.

4.3 The general problem

If the charge distributions do not exhibit any special symmetry about the mid plane then in place of (12) we have

$$F_z = 2\pi^2\epsilon\int \left(K^2|\hat{\phi}_0|^2 - |\hat{\phi}_0'|^2\right)\, dk_x dk_y, \tag{15}$$

since the last $\hat{\phi}_0'$ term no longer vanishes. On substituting $\phi = \phi_S + \phi_A$ in addition to the terms proportional to $|\hat{\phi}_S|^2$ and $|\hat{\phi}_A|^2$ we get a cross term proportional to $\hat{\phi}_S\hat{\phi}_A^* + \hat{\phi}_S^*\hat{\phi}_A$ from the first of the two terms in the integrand of (15), and a term proportional to $\hat{\phi}_S'(\hat{\phi}_A')^* + (\hat{\phi}_S')^*\hat{\phi}_A'$ from the second term. Clearly, since $\hat{\phi}_S'$ and $\hat{\phi}_A$ both vanish on the midplane, the cross terms have a zero contribution to the force. Therefore, the total force may be found simply by summing the right hand sides of (13) and (14). Thus, we have the following general formula for the force normal to the planes:

$$\frac{F_z}{2\pi^2/\epsilon} = \int \left\{\frac{|\hat{\sigma}_S|^2}{\sinh^2(Kh)} - \frac{|\hat{\sigma}_A|^2}{\cosh^2(Kh)}\right\} dk_x dk_y. \tag{16}$$

This is equivalent to the expression for the free energy of a pair of parallel planes with arbitrary charge distribution found by Ben-Yaakov *et al.* [33].

4.4 One dimensional distributions

If $\sigma(x, y)$ is independent of y, the charge distributions are no longer square integrable. Therefore, (16) requires careful interpretion. In order to do this, we write the charge distribution on either plane as

$$\sigma_{\pm}(x, y) = \bar{\sigma}_{\pm}(x)\Delta(y) \tag{17}$$

where $\Delta(y) = 1$ if $|y| < L_y/2$ and $\Delta(y) = 0$ otherwise, L_y being a large but finite length. The Fourier transform of (17) is

$$\hat{\sigma}_{\pm}(k_x, k_y) = \hat{\bar{\sigma}}_{\pm}(k_x)\frac{\sin(k_y L_y/2)}{\pi k_y}, \tag{18}$$

where the caret on $\bar{\sigma}_{\pm}$ now indicates the one dimensional Fourier transform with respect to k_x. Thus, the Fourier transforms of the symmetric and antisymmetric charge densities σ_S and σ_A are also the product of the corresponding 1D transform and the function $\sin(k_y L_y/2)/(\pi k_y)$. Therefore, in the integration with respect to k_y, most of the contribution arises from a zone near the origin of width $\sim \pi/L_y$. Since L_y is large, $K = (\kappa^2 + k_x^2 + k_y^2)^{1/2} \sim (\kappa^2 + k_x^2)^{1/2} \equiv \bar{K}$ and (16) may be expressed as a product of integrals

$$\frac{F_z}{2\pi^2/\epsilon} = \int_{-\infty}^{+\infty} \frac{\sin^2(k_y L_y/2)}{\pi^2 k_y^2}\, dk_y \int_{-\infty}^{+\infty} \left\{ \frac{|\hat{\bar{\sigma}}_S|^2}{\sinh^2(\bar{K}h)} - \frac{|\hat{\bar{\sigma}}_A|^2}{\cosh^2(\bar{K}h)} \right\} dk_x. \tag{19}$$

The first integral on the right-hand side of (19) evaluates to $L_y/(2\pi)$, and thus, if we define the force per unit span, $F = F_z/L_y$, then

$$\frac{F}{\pi/\epsilon} = \int_{-\infty}^{+\infty} \left\{ \frac{|\hat{\sigma}_S|^2}{\sinh^2(Kh)} - \frac{|\hat{\sigma}_A|^2}{\cosh^2(Kh)} \right\} dk, \tag{20}$$

where we have dropped the bar over the σ, a one dimensional Fourier transform with respect to the x-dimension being understood, and k_x, $\bar{K}$ are replaced by k and K respectively. This is what we would have obtained had we simply started by taking a one-dimensional Fourier transform with respect to x in (1).

5 Applications

We now consider some applications of (16) and (20) to special situations where the integral in Fourier space can be evaluated analytically.

5.1 Uniformly charged section of finite length

When two surfaces with like charge interact across a gap of width $2h$, the interaction force decreases exponentially [1] with h as long as $\kappa h \gg 1$. In the opposite limit of $\kappa h \ll 1$ the Debye layers on the two planes are strongly overlapped and the exponential dependence gives way to a power law $\Pi \sim h^{-2}$ at small separations [35], since the potential and ionic number densities are approximately uniform over the gap width and Donnan equilibrium holds [36]. If the charged section of the planes is of finite size ($\sim L$), the charge cloud between the planes tends to spill out ('overspill') beyond this region [24]. This leads to an edge correction to the interaction force which can be non-negligible unless $\kappa L \gg 1$.

We consider two problems. In the first problem the planes are unbounded, with uniform separation $2h$. The charge density on either plane is $\sigma(x) = \sigma_0$ if $|x| < L$ and zero otherwise. Since the planes have infinite extent, the charge cloud of counter ions is confined in the gap $-h < z < h$, though some of it overspills the charged section $|x| < L$. Thus, there is a loss of confinement of the Debye layer in the direction parallel to the planes but not in the normal direction. For brevity, we will call this the "confined problem". In the unconfined problem, the planes are again uniformly charged in the region $|x| < L$, where the gap width is $2h$. However, the planes are of finite extent, and in $|x| > L$ the region $-\infty < z < \infty$ is occupied by electrolyte. The charge cloud of counter ions is confined in $-h < z < h$ in $|x| < L$, but is unconfined where it spills out into $|x| > L$. The two cases are shown schematically in Figure 1.

The unconfined geometry is the more realistic of the two, and has been studied [24] using asymptotic methods that are appropriate only in the limit $\kappa h \ll 1$. The confined problem, though perhaps less realistic, can be solved exactly within the Debye-Hückel limit for any value of κh, and will be studied in detail below. These two problems can be considered as examples of a more general problem in which both the surface charge density and separation between the planes are functions of x.

5.1.1 Like charge

We consider the confined problem in which σ is uniform over a central section and zero elsewhere, with identical distribution on the two planes. The Fourier transform of the charge density is

$$\hat{\sigma}(k) = \frac{1}{2\pi}\int_{-\infty}^{+\infty} \sigma(x)\exp(-ikx)\,dx = \frac{1}{2\pi}\int_{-L}^{+L} \sigma_0\exp(-ikx)\,dx = \frac{\sigma_0}{\pi k}\sin(kL). \qquad (21)$$

Since the charge is symmetric with respect to the midplane in this problem, $\sigma_S = \sigma$ and $\sigma_A = 0$. Thus, from (20), the force on the plane $z = h$ is

$$F = \frac{\sigma_0^2}{\pi\epsilon}\int_{-\infty}^{+\infty} \frac{\sin^2(kL)}{k^2\sinh^2(Kh)}\,dk. \qquad (22)$$

We make a change of variables to $\eta = kL$ in this integral. The disjoining pressure $\Pi = F/(2L)$ is therefore

$$\frac{\Pi}{\sigma_0^2/(2\epsilon)} = \frac{1}{\pi}\int_{-\infty}^{+\infty} \frac{\sin^2\eta}{\eta^2 \sinh^2\left(\kappa h\sqrt{1+\eta^2/\kappa^2L^2}\right)}\, d\eta. \tag{23}$$

The integral on the right may be evaluated numerically for specific pairs of values of κh and κL. It is however instructive to first study some special limits. Taking the limit $\kappa L \to \infty$ in (23) we have

$$\frac{\Pi}{\sigma_0^2/(2\epsilon)} = \frac{\mathrm{cosech}^2(\kappa h)}{\pi}\int_{-\infty}^{+\infty}\frac{\sin^2\eta}{\eta^2}\, d\eta = \mathrm{cosech}^2(\kappa h) = \frac{\Pi_\infty}{\sigma_0^2/(2\epsilon)}, \tag{24}$$

which is the classical result for two uniformly charged infinite planes. Thus, when κh is large, $\Pi_\infty \sim \exp(-2\kappa h)$ corresponding to the weak overlap approximation [1], and when κh is small, $\Pi_\infty \sim (\kappa h)^{-2}$ [35].

We now consider the limit $\kappa h \to 0$ at fixed κL. One may then make the approximation $\sinh x \sim x$ in (23), so that

$$\kappa^2 h^2 \frac{\Pi}{\sigma_0^2/(2\epsilon)} \sim \frac{1}{\pi\kappa L}\int_{-\infty}^{+\infty}\frac{\sin^2(\kappa L\xi)}{\xi^2(1+\xi^2)}\, d\xi. \tag{25}$$

The integral may be evaluated exactly (see Appendix), and thus, we have

$$\frac{\Pi}{\sigma_0^2/(2\epsilon)} \sim \frac{1}{\kappa^2h^2}\left[1 - \frac{1}{2\kappa L}\left\{1-\exp(-2\kappa L)\right\}\right], \quad \kappa h \ll 1. \tag{26}$$

Let us define the force deficit due to edge effects as $\Delta F = 2L(\Pi_\infty - \Pi)$. Then (26) may be expressed as

$$\kappa^2h^2\frac{\Delta F}{\sigma_0^2/(2\epsilon\kappa)} \sim 1 - \exp(-2\kappa L), \quad \kappa h \ll 1. \tag{27}$$

When κL is large, $\Delta F \sim \sigma_0^2/(2\epsilon\kappa^3h^2)$, independent of L. The equivalent of (27) for the unconfined problem is [24]

$$\kappa^2h^2\frac{\Delta F}{\sigma_0^2/(2\epsilon\kappa)} \sim 2\tanh(\kappa L), \quad \kappa h \ll 1. \tag{28}$$

Thus, in the limit of large κL, the force deficit in the unconfined problem is a factor of 2 larger than that for the confined problem. This increase in the force deficit is to be expected, since there is more scope for ions to spill out of the charged central region in the unconfined geometry than in the confined geometry (Figure 1). The force deficits in the confined and unconfined cases are shown in Figure 2. The reduction in the disjoining force is due to the spillage of the Debye charge cloud from the gap between the planes.

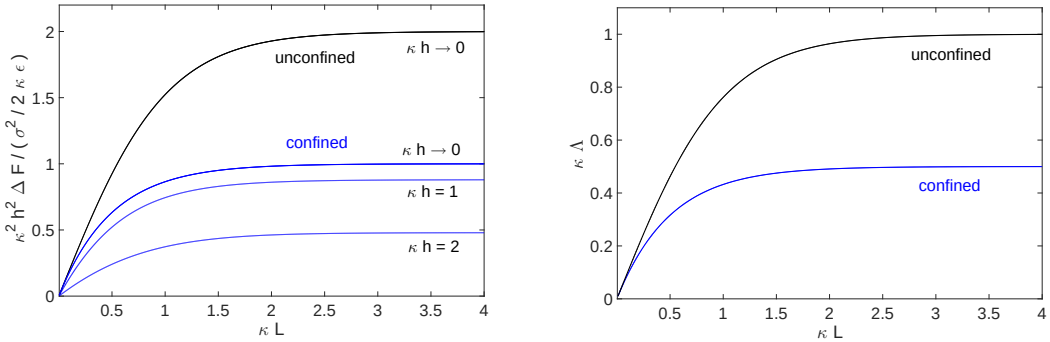

Figure 2: *Left panel:* The normalized force deficit as a function of κL for: (i) the unconfined problem (28) in the limit $\kappa h \to 0$; (ii) the confined problem (27) in the limit $\kappa h \to 0$; (iii) the confined problem (23) with $\kappa h = 1$ and 2. *Right panel:* The normalized lost length $\kappa\Lambda$ as a function of the normalized plate length κL in the limit $\kappa h \to 0$ for: (i) the unconfined problem (30); (ii) the confined problem, (29).

.

The amount of this spillage can be characterized by the "lost length" Λ, defined [24] as the distance along the plane that would normally confine an amount of Debye layer charge equal to the charge Q spilled out beyond one of the edges. For the confined problem, in the limit $\kappa h \to 0$,

$$\Lambda = -\frac{Q}{2\sigma} = \frac{1}{\kappa\,[1 + \coth(\kappa L)]} \tag{29}$$

(see Appendix). From (29) we see that $\Lambda \sim L$ or $\kappa^{-1}/2$ respectively in the limits of short ($\kappa L \ll 1$) and long ($\kappa L \gg 1$) plate lengths. This must be expected, since when the length of the charged section approaches zero, all of the Debye cloud is spilled outside its confines whereas when $L \gg \kappa^{-1}$ only the charge confined within a distance of the order of a Debye length of the edge is lost. In the latter case, the lost charge is a small fraction of the total charge in the counter-ion cloud and the force deficit is also a small correction, independent of L. These results can be compared to the corresponding result [24] for the unconfined problem, for which, in the limit $\kappa h \to 0$,

$$\Lambda = \kappa^{-1} \tanh(\kappa L). \tag{30}$$

The lost lengths for the unconfined and confined problems in the limit $\kappa h \to 0$ are compared in Figure 2. The lost length is smaller in the confined problem which allows less scope for ions to spill out of the gap between the charged sections.

5.1.2 Unlike charge

Let us revisit the problem of a uniformly charged finite section, except that the charges on the two planes are now assumed to be equal and opposite. Thus, $\sigma(x) = \pm\sigma_0$ (corresponding to the planes $z = \pm h$) if $|x| < L$ and zero otherwise. In this case, $\sigma_S = 0$ and $\sigma_A(x) = |\sigma(x)|$. Equation (20) then implies

$$F = -\frac{\pi}{\epsilon}\int_{-\infty}^{+\infty} \frac{|\hat{\sigma}|^2}{\cosh^2(Kh)}\, dk = -\frac{\sigma_0^2}{\epsilon\pi}\int_{-\infty}^{+\infty} \frac{\sin^2(kL)}{k^2\cosh^2(Kh)}\, dk$$
$$= -\frac{\sigma_0^2 L}{\epsilon\pi}\int_{-\infty}^{+\infty} \frac{\sin^2\eta}{\eta^2\cosh^2\left(\kappa h\sqrt{1+\eta^2/\kappa^2L^2}\right)}\, d\eta. \tag{31}$$

Thus, the disjoining pressure, $\Pi = F/(2L)$ in this case is

$$\frac{\Pi}{\sigma_0^2/(2\epsilon)} = -\frac{1}{\pi}\int_{-\infty}^{+\infty} \frac{\sin^2\eta}{\eta^2\cosh^2\left(\kappa h\sqrt{1+\eta^2/\kappa^2L^2}\right)}\, d\eta. \tag{32}$$

The disjoining pressure is negative (attractive interaction), and can be evaluated by numerical integration for any pair of values of κh and κL. However, we again first study some special limits. Taking the limit $\kappa L \to \infty$ in (32) we have

$$-\frac{\Pi}{\sigma_0^2/(2\epsilon)} = \frac{\mathrm{sech}^2(\kappa h)}{\pi}\int_{-\infty}^{+\infty} \frac{\sin^2\eta}{\eta^2}\, d\eta = \mathrm{sech}^2(\kappa h) = -\frac{\Pi_\infty}{\sigma_0^2/(2\epsilon)} \tag{33}$$

for two uniformly charged infinite planes with unlike charge. In this case, $\Pi_\infty \sim \exp(-2\kappa h)$ when κh is large but in the limit of vanishing separation, $\kappa h \to 0$, we have a finite disjoining pressure.

5.2 Two dimensional periodic distributions

Let us now suppose that we have a charge distribution $\sigma(x, y)$ that is a periodic function of x and y. With no loss of generality we may assume that the charge distribution is generated by specifying it in a finite domain $D_0 = [-L_x/2, L_x/2] \times [-L_y/2, L_y/2]$ which is then repeated $(2N + 1)$ times in the x and y directions. The value of σ is taken as zero outside the $(2N+1)L_x \times (2N+1)L_y$ sized rectangular region. Thus, $\sigma(x, y)$ is of compact support and square integrable. We will of course pass to the limit $N \to \infty$ in the final answer; we will call D_0 the primitive cell.

We temporarily suppress the subscript 'S' or 'A' and simply use σ for the charge

distribution. On account of the periodicity we have

$$\hat{\sigma}(k_x,k_y)=\tilde{\sigma}(k_x,k_y)\frac{L_xL_y}{(2\pi)^2}\sum_{m=-N}^{+N}\sum_{n=-N}^{+N}\exp[-i(mk_xL_x+nk_yL_y)]$$
$$=\tilde{\sigma}(k_x,k_y)\frac{L_xL_y}{(2\pi)^2}g\left(\frac{k_xL_x}{2}\right)g\left(\frac{k_yL_y}{2}\right). \tag{34}$$

Here $\tilde{\sigma}$ is defined as

$$\tilde{\sigma}(k_x,k_y)=\frac{1}{L_xL_y}\int_{D_0}\sigma(x,y)\exp[-i(k_xx+k_yy)]\,dxdy \tag{35}$$

and the function

$$g(\xi)=\sum_{m=-N}^{+N}\exp(-2im\xi)=\frac{\sin\{(2N+1)\xi\}}{\sin\xi}. \tag{36}$$

The function $g(\xi)$ has the following properties when N is large: (i) when $\xi\to\xi_k=k\pi$ $(k=0,\pm1,\pm2,\cdots)$, $g(\xi)\to 2N+1$, (ii) for all other values $g(\xi)$ oscillates rapidly about zero with an amplitude of order unity, (iii) the integral of the square of $g(\xi)$ in the neighborhood of ξ_k is $(2N+1)\pi$. Indeed,

$$\int_{\xi_k-0}^{\xi_k+0}g^2(\xi)\,d\xi\sim\int_{-\infty}^{+\infty}\frac{\sin^2\{(2N+1)(\xi-\xi_k)\}}{(\xi-\xi_k)^2}\,d\xi=(2N+1)\int_{-\infty}^{+\infty}\frac{\sin^2 x}{x^2}\,dx=(2N+1)\pi. \tag{37}$$

Thus, in the neighborhood of $\xi=\xi_k$, in the limit $N\to\infty$.

$$g^2(\xi)\to\pi(2N+1)\delta(\xi-\xi_k) \tag{38}$$

where δ denotes the Dirac delta function. Let us define the reciprocal lattice as a set of wave vectors $\boldsymbol{\rho}=\hat{\boldsymbol{i}}(2\pi m/L_x)+\hat{\boldsymbol{j}}(2\pi n/L_y)$ where $m,n=0,\pm1,\pm2,\pm3,\cdots$. Then at any neighborhood of a reciprocal lattice vector,

$$g^2\left(\frac{k_xL_x}{2}\right)g^2\left(\frac{k_yL_y}{2}\right)=\pi^2(2N+1)^2\delta\left(\frac{k_xL_x}{2}-m\pi\right)\delta\left(\frac{k_yL_y}{2}-n\pi\right)$$
$$\to\frac{4\pi^2(2N+1)^2}{L_xL_y}\delta(\boldsymbol{k}-\boldsymbol{\rho}). \tag{39}$$

Thus, the integral in (16) reduces to a sum over the reciprocal lattice and we have for the disjoining pressure

$$\Pi=\frac{F_z}{L_xL_y(2N+1)^2}=\frac{1}{2\epsilon}\sum_{\boldsymbol{\rho}}\left[\frac{|\tilde{\sigma}_S|^2}{\sinh^2(Kh)}-\frac{|\tilde{\sigma}_A|^2}{\cosh^2(Kh)}\right] \tag{40}$$

where $K = (\kappa^2 + \rho^2)^{1/2}$.

A uniformly charged plate may be considered a periodic charge with the period $L_x, L_y \to \infty$. In this case, the reciprocal lattice contains only the single point $\boldsymbol{\rho} = 0$ where $\tilde{\sigma}(k_x, k_y) = \sigma_0$. Thus, from (40), $\Pi = \Pi_{\rm sym} = (\sigma_0^2/2\epsilon)\,\mathrm{cosech}^2(\kappa h)$ in the symmetric case and $\Pi = \Pi_{\rm asym} = -(\sigma_0^2/2\epsilon)\,\mathrm{sech}^2(\kappa h)$ in the anti-symmetric case, as expected.

5.2.1 Zebra stripes

Let us suppose that we have charged stripes of width δ parallel to the y-axis separated by uncharged sections of width Δ. In this case, the primitive cell may be taken as the domain $[-L_x/2, L_x/2] \times [-L_y/2, L_y/2]$ where $L_x = \delta + \Delta = L$ and $L_y \to \infty$. The interval $-\delta/2 > x > \delta/2$ carries a charge density σ_0 and the remainder of the cell has zero charge. The reciprocal lattice then consists of the vectors $\boldsymbol{\rho} = \hat{\boldsymbol{\imath}}(2\pi/L)n$, where $n = 0, \pm 1, \pm 2, \cdots$, and,

$$\tilde{\sigma}(\boldsymbol{\rho}) = \frac{\sigma_0}{L}\int_{-\delta/2}^{\delta/2} \exp\left(-2n\pi i\frac{x}{L}\right)\,dx = \frac{\sigma_0}{n\pi}\sin\left(\frac{n\pi\delta}{L}\right). \tag{41}$$

On substituting in (40), we have in the symmetric case

$$\frac{\Pi_{\rm sym}}{\sigma_0^2/(2\epsilon)} = \frac{\delta^2}{L^2}\,\mathrm{cosech}^2(\kappa h) + \sum_{n=1}^{\infty}\frac{2}{n^2\pi^2}\sin^2\left(\frac{n\pi\delta}{L}\right)\mathrm{cosech}^2\left(\kappa h\sqrt{1+\frac{4\pi^2n^2}{\kappa^2L^2}}\right), \tag{42}$$

and in the antisymmetric case

$$-\frac{\Pi_{\rm asym}}{\sigma_0^2/(2\epsilon)} = \frac{\delta^2}{L^2}\,\mathrm{sech}^2(\kappa h) + \sum_{n=1}^{\infty}\frac{2}{n^2\pi^2}\sin^2\left(\frac{n\pi\delta}{L}\right)\mathrm{sech}^2\left(\kappa h\sqrt{1+\frac{4\pi^2n^2}{\kappa^2L^2}}\right). \tag{43}$$

Note that if $\Delta \to 0$, $\delta \to L$ and in this case we recover the result for the disjoining pressure between uniformly charged planes.

5.2.2 Zebra stripes with alternating charge

Instead of having positively charged stripes separated by uncharged regions, let us now suppose that we have alternate bands of positive charge (surface density σ_0, width Δ_+) and negative charge (surface density $-\sigma_0$, width Δ_-). The primitive cell once again is of width $L = \Delta_+ + \Delta_-$, of which the central region $(-\Delta_+/2, \Delta_+/2)$ carries a surface charge density of σ_0 with the remainder of the cell carrying $-\sigma_0$. As before, $L_y = \infty$. Thus,

$$\begin{aligned}\tilde{\sigma}(\boldsymbol{\rho}) &= \frac{\sigma_0}{L}\left(\int_{-\Delta_+/2}^{\Delta_+/2} - \int_{-L/2}^{-\Delta_+/2} - \int_{\Delta_+/2}^{L/2}\right)e^{-2in\pi x/L}\,dx \\ &= \frac{\sigma_0}{L}\begin{cases}\Delta_+ - \Delta_- & \text{if } n = 0,\\ (2L/n\pi)\sin(n\pi\Delta_+/L) & \text{if } n > 0.\end{cases}\end{aligned} \tag{44}$$

On substituting in (40), we have in the symmetric case

$$\frac{\Pi_{\rm sym}}{\sigma_0^2/(2\epsilon)} = \left(\frac{\Delta_+ - \Delta_-}{\Delta_+ + \Delta_-}\right)^2 \operatorname{cosech}^2(\kappa h) + \sum_{n=1}^{\infty} \frac{8\sin^2(n\pi\Delta_+/L)}{n^2\pi^2 \sinh^2\left(\kappa h\sqrt{1+\frac{4\pi^2 n^2}{\kappa^2 L^2}}\right)}, \tag{45}$$

and in the antisymmetric case

$$-\frac{\Pi_{\rm asym}}{\sigma_0^2/(2\epsilon)} = \left(\frac{\Delta_+ - \Delta_-}{\Delta_+ + \Delta_-}\right)^2 \operatorname{sech}^2(\kappa h) + \sum_{n=1}^{\infty} \frac{8\sin^2(n\pi\Delta_+/L)}{n^2\pi^2 \cosh^2\left(\kappa h\sqrt{1+\frac{4\pi^2 n^2}{\kappa^2 L^2}}\right)}. \tag{46}$$

Note that if either $\Delta_+ = 0$ or $\Delta_- = 0$, the result for uniformly charged planes is recovered. Further note that if $\Delta_+ = \Delta_-$ then both planes are overall charge neutral. In this case, the first terms in (45) and (46) vanish. But since $\operatorname{cosech} x > \operatorname{sech} x$, each term in the series (45) exceeds in magnitude the corresponding term in the series (46). Thus,

$$|\Pi_{\rm sym}| > |\Pi_{\rm asym}| \tag{47}$$

in agreement with [33].

5.2.3 Checker board pattern

We now consider a "checker board pattern" where each square is of edge length Δ and alternate cells have charge density $\pm\sigma_0$. The primitive cell may then be taken as a square of edge length 2Δ divided into four subunits. The first and third quadrants carry a charge density σ_0 whereas the remaining quadrants carry a charge density $-\sigma_0$. The reciprocal lattice consists of the vectors $\boldsymbol{\rho} = \hat{\boldsymbol{i}}(m\pi/\Delta) + \hat{\boldsymbol{j}}(n\pi/\Delta)$ where $m, n = 0, \pm1, \pm2, \cdots$. A straightforward calculation shows that

$$\tilde{\sigma}(\boldsymbol{\rho}) = \begin{cases} -4\sigma_0/\pi^2 mn & \text{if } m \text{ and } n \text{ are odd,} \\ 0 & \text{otherwise.} \end{cases} \tag{48}$$

On substituting in (40), we have in the symmetric case

$$\frac{\Pi_{\rm sym}}{\sigma_0^2/(2\epsilon)} = \frac{64}{\pi^4} \sum_{\substack{m,n=1 \\ m,n \text{ odd}}}^{\infty} \frac{1}{m^2 n^2} \operatorname{cosech}^2\left(\kappa h\sqrt{1+\frac{\pi^2}{\kappa^2\Delta^2}(m^2+n^2)}\right). \tag{49}$$

The antisymmetric case corresponds to shifting the planes relative to each other in either the x or y directions by the amount Δ. The disjoining pressure in this case is negative and we have

$$-\frac{\Pi_{\rm asym}}{\sigma_0^2/(2\epsilon)} = \frac{64}{\pi^4} \sum_{\substack{m,n=1 \\ m,n \text{ odd}}}^{\infty} \frac{1}{m^2 n^2} \operatorname{sech}^2\left(\kappa h\sqrt{1+\frac{\pi^2}{\kappa^2\Delta^2}(m^2+n^2)}\right). \tag{50}$$

5.2.4 Point charges on square lattice

Let us consider a two dimensional array of point charges, Q, located at the nodes of a square lattice of spacing Δ. This could be a representation of the discrete nature of the charge distribution on surfaces when viewed on atomic scales. Here the primitive cell may be taken as the square $[-\Delta/2, \Delta/2] \times [-\Delta/2, \Delta/2]$ with a charge Q at the origin. The reciprocal lattice consists of the vectors $\boldsymbol{\rho} = \hat{\boldsymbol{i}}(2\pi m/\Delta) + \hat{\boldsymbol{j}}(2\pi n/\Delta)$ where $m, n = 0, \pm 1, \pm 2, \cdots$, and

$$\tilde{\sigma}(\boldsymbol{\rho}) = \frac{1}{\Delta^2} \int_{D_0} Q\delta(\boldsymbol{r}) e^{-i\boldsymbol{\rho}\cdot\boldsymbol{r}} \, d^2\boldsymbol{r} = \frac{Q}{\Delta^2}. \tag{51}$$

On substituting in (40), we have in the symmetric case

$$\frac{\Pi_{\text{sym}}}{\sigma_0^2/(2\epsilon)} = \operatorname{cosech}^2(\kappa h) + \sum_{m,n=1}^{\infty} 4 \operatorname{cosech}^2 \left(\kappa h \sqrt{1 + \frac{4\pi^2}{\kappa^2\Delta^2}(m^2+n^2)} \right), \tag{52}$$

where $\sigma_0 = Q/\Delta^2$ is the average charge density. The anti-symmetric case is also interesting as it describes, for example, a surface with a discrete charge distribution approaching a conducting plane. The corresponding result for the disjoining pressure is

$$-\frac{\Pi_{\text{asym}}}{\sigma_0^2/(2\epsilon)} = \operatorname{sech}^2(\kappa h) + \sum_{m,n=1}^{\infty} 4 \operatorname{sech}^2 \left(\kappa h \sqrt{1 + \frac{4\pi^2}{\kappa^2\Delta^2}(m^2+n^2)} \right). \tag{53}$$

Some limiting cases are of interest. Suppose that $\Delta \ll \kappa^{-1}, h$. In this case, the double sums in (52) and (53) vanish and the case of uniformly charged planes is recovered. Since each of the terms being summed is positive, discreteness of charge always has the effect of increasing the magnitude of the interaction. The dependence of the disjoining pressure on κh and $\kappa\Delta$ is shown in Figure 3.

5.3 Two dimensional random distributions

We now consider two parallel infinite planes with charge distributions $\sigma_\pm = \sigma_{0\pm} + \sigma_{f\pm}$, where the $\sigma_{f\pm}$ are random distributions with zero mean and finite variance. As in Section 44.3, we construct the symmetric and antisymmetric combinations $\sigma_S = (\sigma_+ + \sigma_-)/2$ and $\sigma_A = (\sigma_+ - \sigma_-)/2$. The disjoining pressure is then given by (16) in terms of $\langle|\hat{\sigma}_S|^2\rangle$ and $\langle|\hat{\sigma}_A|^2\rangle$, where $\langle\ \rangle$ indicates an average over a suitable statistical ensemble. The force is therefore the sum of that due to uniform symmetric and antisymmetric charge distributions $\langle\sigma_S\rangle$ and $\langle\sigma_A\rangle$, together with contributions from the fluctuations. In the following sections we therefore consider symmetric and antisymmetric charge distributions with zero mean and variance $\langle\sigma_S^2\rangle$ or $\langle\sigma_A^2\rangle$.

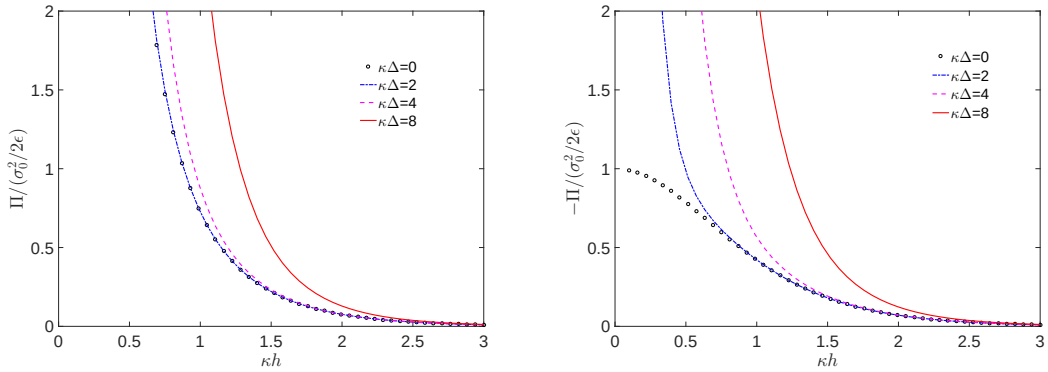

Figure 3: Normalized disjoining pressure between a pair of flat surfaces with discrete point charges on a square lattice as a function of the dimensionless plate separation (κh) for fixed values of the normalized lattice spacing ($\kappa\Delta$). The symmetric (left) and antisymmetric (right) cases are shown. The limit $\kappa\Delta = 0$ corresponds to a uniform distribution with no granularity.

5.3.1 Symmetric problem

We first consider the symmetric problem characterized by a two point autocorrelation

$$\mathcal{C}(\rho) = \frac{\langle \sigma_S(x,y)\sigma_S(x',y')\rangle}{\langle \sigma_S^2\rangle}, \tag{54}$$

where $\rho = [(x-x')^2 + (y-y')^2]^{1/2}$. Our assumption that the system is homogeneous and isotropic cannot hold if the charged regions are of finite lateral extent. Thus, we must assume that the characteristic size L of the charged domain D_0 is much larger than the correlation length α^{-1} characterizing the distance over which the function $\mathcal{C}(\rho)$ decays to zero, and eventually pass to the limit $\alpha L \to \infty$. Equation (13) can be written in terms of the ensemble average as

$$F_z = \frac{2\pi^2}{\epsilon}\int \langle|\hat{\sigma}_S|^2\rangle \,\mathrm{cosech}^2(Kh)\; dk_x dk_y, \tag{55}$$

and $\langle|\hat{\sigma}_S|^2\rangle$ may be expressed in terms of the two point correlation as

$$\langle|\hat{\sigma}_S|^2\rangle = \frac{1}{(2\pi)^4}\int_{D_0} dx\, dy \int_{D_0} dx'\, dy' \langle\sigma_S(x,y)\sigma_S(x',y')\rangle \exp(-i\boldsymbol{k}\cdot\boldsymbol{\rho}), \tag{56}$$

where $\boldsymbol{\rho}$ is the vector that points from (x,y) to (x',y'). Introducing the two point correlation (54) into (56) we obtain, from (55),

$$\Pi = \frac{F_z}{A} = \frac{\langle\sigma_S^2\rangle}{2\epsilon}\frac{1}{(2\pi)^2}\int\left\{\int \mathcal{C}(\rho)\exp(-i\boldsymbol{k}\cdot\boldsymbol{\rho})\, d\boldsymbol{\rho}\right\}\mathrm{cosech}^2(Kh)\; dk_x dk_y, \tag{57}$$

where A is the area of the charged domain D_0, and the integration with respect to $\boldsymbol{\rho}$ extends over the infinite (x, y) plane. The latter integral can be split into angular and radial components, with the angular integral expressible in terms of the Bessel function $J_0(k\rho)$. Thus,

$$\frac{\Pi}{\langle\sigma_S^2\rangle/(2\epsilon)} = \int_0^\infty \left\{ \int_0^\infty \rho\, \mathcal{C}(\rho) J_0(k\rho)\, d\rho \right\} k\, \mathrm{cosech}^2(Kh)\, dk. \tag{58}$$

If we express the two point correlation as $\mathcal{C}(\rho) = \mathcal{C}_0(\alpha\rho)$ where $\mathcal{C}_0$ is parameter free and α^{-1} is the correlation length, then (58), rewritten using dimensionless variables $\bar{\rho} = \alpha\rho$ and $\bar{k} = k/\alpha$, becomes

$$\frac{\Pi}{\langle\sigma_S^2\rangle/(2\epsilon)} = \int_0^\infty \left\{ \int_0^\infty \bar{\rho}\, \mathcal{C}_0(\bar{\rho}) J_0(\bar{\rho}\bar{k})\, d\bar{\rho} \right\} \bar{k}\, \mathrm{cosech}^2 \left(\kappa h \sqrt{1 + \frac{\alpha^2}{\kappa^2}\bar{k}^2} \right) d\bar{k}. \tag{59}$$

Thus, the dimensionless disjoining pressure is a function of the two independent dimensionless parameters κh and α/κ. Two special limits are of interest.

Long correlation length Let us consider the situation where the correlation length greatly exceeds the Debye length, i.e. $\alpha^{-1} \gg \kappa^{-1}$. The term α^2/κ^2 in (59) may now be neglected, leaving

$$\frac{\Pi}{\langle\sigma_S^2\rangle/(2\epsilon)} = \mathrm{cosech}^2(\kappa h) \int_0^\infty \left\{ \int_0^\infty \bar{\rho}\, \mathcal{C}_0(\bar{\rho}) J_0(\bar{\rho}\bar{k})\, d\bar{\rho} \right\} \bar{k}\, d\bar{k}. \tag{60}$$

The double integral on the right hand side of the equation evaluates to $\mathcal{C}_0(0) = 1$. To see this, we either appeal to the Hankel transform pair $(1, \delta(\bar{\rho})/\bar{\rho})$, or we interchange the order of integration after introducing a regularizing factor $\exp(-a\bar{k})$ in the integrand. The integral with respect to $\bar{k}$ can be evaluated exactly,

$$\int_0^\infty \bar{k} e^{-a\bar{k}} J_0(\bar{\rho}\bar{k})\, d\bar{k} = \frac{a}{(a^2 + \bar{\rho}^2)^{3/2}}, \tag{61}$$

by parametric differentiation with respect to a of the standard integral [37]

$$\int_0^\infty e^{-ax} J_0(bx)\, dx = \frac{1}{\sqrt{a^2 + b^2}}. \tag{62}$$

On substituting (61) in (60) and changing variables to $\xi = \bar{\rho}/a$, the integral becomes

$$\int_0^\infty \frac{\xi \mathcal{C}_0(a\xi)\, d\xi}{(1 + \xi^2)^{3/2}} \to \mathcal{C}_0(0) \int_0^\infty \frac{\xi\, d\xi}{(1 + \xi^2)^{3/2}} = \mathcal{C}_0(0) = 1, \tag{63}$$

on taking the limit $a \to 0$. Thus, in the limit of long correlation length,

$$\frac{\Pi}{\langle\sigma_S^2\rangle/(2\epsilon)} = \mathrm{cosech}^2(\kappa h), \tag{64}$$

the same as (24) for parallel planes with uniform charge $\langle\sigma_S^2\rangle^{1/2}$ on each surface, and independent of the functional form of the two point correlation function.

Short correlation length When the fluctuations in the charge are very fine grained, with $\alpha^{-1} \ll \kappa^{-1}$, we introduce the small parameter $\delta = \kappa/\alpha$, and the rescaled variable $\eta = \bar{k}/\delta = k/\kappa$ in (59):

$$\frac{\Pi}{\langle\sigma_S^2\rangle/(2\epsilon)} = \delta^2 \int_0^\infty \left\{ \int_0^\infty \bar{\rho}\, \mathcal{C}_0(\bar{\rho}) J_0(\delta\bar{\rho}\eta)\, d\bar{\rho} \right\} \eta\, \mathrm{cosech}^2\left(\kappa h\sqrt{1+\eta^2}\right)\, d\eta. \tag{65}$$

In the limit $\delta \to 0$, $J_0(\delta\bar{\rho}\eta) \to 1$ and therefore

$$\frac{\Pi}{\langle\sigma_S^2\rangle/(2\epsilon)} = \frac{\beta\kappa^2}{\alpha^2}\mathcal{F}(\kappa h), \tag{66}$$

where

$$\beta = \frac{1}{2}\int_0^\infty \bar{\rho}\,\mathcal{C}_0(\bar{\rho})\, d\bar{\rho} \tag{67}$$

is a constant of order unity, and the function $\mathcal{F}(x)$ is defined as

$$\mathcal{F}(x) = \int_0^\infty \frac{2\eta\, d\eta}{\sinh^2(x\sqrt{1+\eta^2})} = \frac{2}{x^2}\int_x^\infty \frac{t\, dt}{\sinh^2 t} = \frac{2}{x^2}\left[x\coth x - \ln(\sinh x) - \ln 2\right], \tag{68}$$

$$= \frac{2}{x^2}\left[\ln(x^{-1}) + 1 - \ln 2 + \cdots\right], \qquad 0 < x \ll 1, \tag{69}$$

$$\sim \frac{4}{x}e^{-2x}, \qquad x \gg 1. \tag{70}$$

Thus, the disjoining pressure (66) decreases as α^{-2} as $\alpha \to \infty$ (i.e. as the correlation length α^{-1} becomes smaller).

Intermediate correlation length If the correlation length α^{-1} is neither long nor short compared to the Debye length κ^{-1}, we determine the disjoining pressure by evaluating the integral in (59). As an example, we consider a two point correlation function of the form

$$\mathcal{C}(\rho) = \exp(-\alpha\rho). \tag{71}$$

Thus, $\mathcal{C}_0(\bar{\rho}) = \exp(-\bar{\rho})$ and from (67), $\beta = 1/2$. The integral with respect to $\bar{\rho}$ in (59) may be obtained in closed form using (61), thus

$$\frac{\Pi}{\langle\sigma_S^2\rangle/(2\epsilon)} = \int_0^\infty \frac{\bar{k}}{(1+\bar{k}^2)^{3/2}}\,\mathrm{cosech}^2\left(\kappa h\sqrt{1+\frac{\alpha^2}{\kappa^2}\bar{k}^2}\right)\, d\bar{k}. \tag{72}$$

The integral in (72) was evaluated numerically and Figure 4 shows the resulting normalized disjoining pressure as a function of α/κ. Also shown are the asymptotic limits at long correlation lengths, (64), and short correlation lengths, (66).

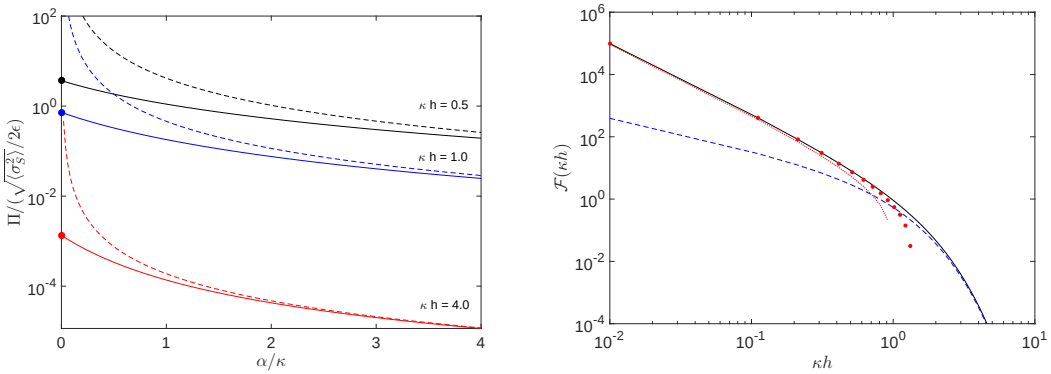

Figure 4: *Left panel*: The normalized disjoining pressure from (72) for the autocorrelation (71), for fixed values of κh as a function of α/κ (solid lines). The corresponding dashed lines are the short correlation length ($\alpha/\kappa \gg 1$) asymptotic approximation (66). The filled circles are the long correlation length limit ($\alpha/\kappa \to 0$) (64). *Right panel*: The function $\mathcal{F}(\kappa h)$ given by (68) (solid line). Also shown are the large argument approximation (70) (dashed line) and the one (dotted line) and two term (filled circles) small argument asymptotic approximation (69).

5.3.2 Antisymmetric problem

In the case of an antisymmetric charge distribution (58) is replaced by

$$\frac{\Pi}{\langle\sigma_A^2\rangle/(2\epsilon)} = -\int_0^\infty \left\{\int_0^\infty \rho\, \mathcal{C}(\rho) J_0(k\rho)\, d\rho\right\} k\,\mathrm{sech}^2(Kh)\, dk. \tag{73}$$

At long correlation lengths we get the classical result (33) for uniform plates with charge density $\langle\sigma_A^2\rangle^{1/2}$, i.e. $\Pi = -(\langle\sigma_A^2\rangle/2\epsilon)\,\mathrm{sech}^2(\kappa h)$, and at short correlation lengths

$$\frac{\Pi}{\langle\sigma_A^2\rangle/(2\epsilon)} = -\frac{\beta\kappa^2}{\alpha^2}\mathcal{G}(\kappa h), \tag{74}$$

where

$$\mathcal{G}(x) = \frac{2}{x^2}\int_x^\infty \frac{t\,dt}{\cosh^2 t} = \frac{2}{x^2}\left[\ln 2 - x\tanh x + \ln\cosh(x)\right]. \tag{75}$$

When x is large, $\mathcal{G}(x) \sim \mathcal{F}(x) \sim (4/x)\exp(-2x)$. When x is small, $\mathcal{G}(x) \sim 2\ln(2)/x^2$. For the special choice (71) of the two point correlation function, the dimensionless disjoining pressure in the antisymmetric problem becomes

$$\frac{\Pi}{\langle\sigma_A^2\rangle/(2\epsilon)} = -\int_0^\infty \frac{\bar{k}}{(1+\bar{k}^2)^{3/2}}\,\mathrm{sech}^2\left(\kappa h\sqrt{1+\frac{\alpha^2}{\kappa^2}\bar{k}^2}\right)\, d\bar{k} \tag{76}$$

which may be compared with the result (72) for the symmetric case.

5.3.3 General problem

By way of example, we consider two plates, each with zero net charge, and with no cross-correlation between the charge distributions on the two plates. Thus, $\langle\sigma_+\rangle = \langle\sigma_-\rangle = \langle\sigma_+\sigma'_-\rangle = 0$, where the prime indicates evaluation at (x', y') rather than (x, y). Let us also suppose that the mean squared charge density is $\langle\sigma^2\rangle$ and the autocorrelation is $\mathcal{C}(\rho)$ on either plate. Thus, $\langle\sigma_+^2\rangle = \langle\sigma_-^2\rangle = \langle\sigma^2\rangle$ and $\langle\sigma_+\sigma'_+\rangle = \langle\sigma_-\sigma'_-\rangle = \langle\sigma^2\rangle\mathcal{C}(\rho)$. It follows that $\langle\sigma_S\sigma'_S\rangle = \langle\sigma_A\sigma'_A\rangle = \langle\sigma^2\rangle\mathcal{C}(\rho)/2$, i.e. the autocorrelations of σ_S and σ_A are non-zero, even though the charge distributions on the two plates are uncorrelated. Thus, on combining (58) and (73) we have

$$\frac{\Pi}{\langle\sigma^2\rangle/(2\epsilon)} = \int_0^\infty \left\{ \int_0^\infty \rho\, \mathcal{C}(\rho) J_0(k\rho)\, d\rho \right\} 2k\, \mathrm{cosech}^2(2Kh)\, dk. \tag{77}$$

Note that the disjoining pressure is non-zero even though the charge fluctuations on the two plates are uncorrelated with each other. This is because interactions between elements with like charge and unlike charge do not contribute equally to the total force. Velegol and Thwar [38] concluded that planes with random, uncorrelated charge attract each other, rather than repel. However, their analysis differs from ours in two respects. (i) They assume a force law at each point (x, y) that is identical to that between planes with uniform charge. This neglects the tendency of the charge cloud to smooth itself out over the Debye length scale κ^{-1}, and is therefore unsatisfactory when the correlation length is small compared to the Debye length. (ii) More importantly, they assume that the potentials on the planes (rather than the surface charge densities) are held constant, leading to a different force law [21].

6 Discussion

We have presented explicit formulas for the disjoining pressure between inhomogeneously charged planes for various charge distributions that should be useful in applications.Though our starting point, (9), is not restricted to low potentials, in the subsequent development we have adopted the Debye-Huckel linearized theory in order to derive expressions for the disjoining pressure. It is, however, well known that the Debye-Huckel linearized theory is inadequate when potentials on charged surfaces exceed the thermal scale $k_BT/e \approx 25$ mV. This is particularly relevant when the surfaces are very close together ($\kappa h \ll 1$), as in this case Debye shielding is ineffective at reducing the potentials near the surfaces.

This nonlinear regime can be explored by perturbation methods or by numerical solution of the underlying Poisson-Boltzmann equation [31, 39]. However, if the surface charge density is very large, the disjoining pressure can be obtained by a minor modification of the method presented here. By 'very large' we mean that the surface charge density, σ, greatly exceeds the critical charge density, $\sigma_c = e/(\ell_B\kappa^{-1})$ where $\ell_B = e^2/(4\pi\epsilon k_BT)$ is the Bjerrum length. This critical density corresponds to the presence of one electronic charge for every

square of side $h = (\ell_B/\kappa)^{1/2}$, the geometric mean of the Debye length and Bjerrum length. When $\sigma \gg \sigma_c$, the Debye layer may be regarded as an inner layer where the potential is comparable to the thermal scale, and an outer diffuse layer where the Debye-Hückel approximation may be employed. The extent of this inner layer is defined by the length scale $\ell = \kappa^{-1} \ln(2\pi z\sigma/\sigma_c)$, for a symmetric electrolyte with valence z. If σ/σ_c is sufficiently large that ℓ is much less than each of the other three length scales κ^{-1}, h and L then the geometry of the nonlinear region may be regarded as planar. In this situation, an exact solution of the Poisson Boltzmann equation is available for a binary symmetric electrolyte and can be matched to the outer diffuse layer. This matching procedure is well known [1] and leads to the conclusion that in the far field the classical linear Debye-Hückel solution is valid provided one replaces the true charge density, σ, by an "effective" or "renormalized" charge density $\sigma_e = (\sigma_c/\pi z) \ln(2\pi z\sigma/\sigma_c)$. Thus, all of the results presented in this paper may be used but with σ replaced by the corresponding σ_e at all points on the surface.

In this paper we have neglected any penetration of the electric fields into the dielectric substrate bounding the electrolyte. Since the relative permittivity of water is very large compared to that of common substrates (e.g. plastics, glass, lipids etc.), this neglect is usually a very good approximation except in special situations such as near dielectric-electrolyte interfaces with sharp corners [40]. However, this assumption is not essential to the development presented here and can be avoided by replacing (8) by a potential that is continuous at the interface between the electrolyte and the dielectric substrate, with a jump in derivative corresponding to the surface charge at the interface. The finite permittivity contrast between electrolyte and dielectric will cause some flux leakage into the solid which will alter the calculation of the edge effect in a non-trivial manner. Under appropriate conditions, this correction may be significant. We leave an investigation of this to future work.

7 Conclusion

We have presented a method for calculating the normal force between inhomogeneously charged planes bounding an electrolyte. The problem was considered within the linearized Debye-Hückel approximation that is valid when the electric potentials everywhere are small compared to the thermal scale k_BT/e. This problem has been considered by various authors (see Sec. 1) in different contexts starting with the work of Richmond [30, 32]. In all cases, the basic approach involved developing an expression for the free energy by the "charging method" discussed by Richmond. This has the advantage that the free energy is a scalar, and once it is known all force components can be determined by differentiation. We have presented here an alternate approach that may be much more efficient if one is only interested in the normal component of the interaction force (disjoining pressure). We have applied this method to the various classes of problems and in each case we have presented explicit formulas for the disjoining pressure that should be useful in applications.

A distribution that appears not to have been considered before is that of a pair of infinite planes with a central charged section. This configuration is interesting because it provides a simple model for understanding the effects of loss of lateral confinement of the Debye layer. Previous work [24] considered Debye layer overspill out of the gap between two dielectric blocks that face each other across a gap of width $2h$ and are of lateral extent $2L$. An analysis was presented in the Debye-Hückel limit for the case of Debye length (κ^{-1}) much greater than h. This block geometry ('unconfined') and the case of infinite parallel planes ('confined') considered here may be regarded as special cases of a general one dimensional problem in which the gap width $2h(x)$ and charge densities $\sigma = \sigma_{\pm}(x)$ are functions of position x. These special cases have enabled us to demonstrate the effects of charge overspill in problems that are sufficiently simple that analytic expressions can be obtained for the consequent reduction in the force between the charged surfaces. In conclusion, we point out that the "confined" problem studied here is similar in some ways to the problem of electro-osmotic flow past a step change in surface charge considered by Yariv [41].

Acknowledgement

We thank an anonymous referee for suggesting improvements to Sec. 55.3. J.D.S. thanks the Department of Applied Mathematics & Theoretical Physics, University of Cambridge, for hospitality.

Appendix A: Derivation of (26) and (29)

Using $\bar{\phi}(x)$ to denote the average of the potential $\phi(x,z)$ over the channel cross-section, z, we have, from (1) and (2), $\partial_{xx}\bar{\phi} - \kappa^2\bar{\phi} = -\sigma_0/\epsilon h$ if $|x| < L$ and zero otherwise. Solutions are symmetric about $x = 0$ and take the form

$$\bar{\phi}(x) = \begin{cases} \sigma_0/(\epsilon\kappa^2 h) + A\cosh(\kappa x) & \text{if } |x| \le L, \\ B\exp(-\kappa|x|) & \text{if } |x| > L. \end{cases} \tag{78}$$

Continuity of $\bar{\phi}$ and $\partial_x\bar{\phi}$ at $x = L$ determines the constants A and B:

$$A = -\frac{\sigma_0\exp(-\kappa L)}{\epsilon\kappa^2 h}, \qquad B = \frac{\sigma_0\sinh(\kappa L)}{\epsilon\kappa^2 h}. \tag{79}$$

In the limit $\kappa h \ll 1$, $\phi(x,z) \sim \bar{\phi}(x) + O(\kappa^2 h^2)$, and thus, from (9),

$$\Sigma_{zz} \sim -\frac{\epsilon}{2}\begin{cases} 2B^2\kappa^2\exp(-2\kappa|x|) & \text{if } |x| > L, \\ \frac{\sigma_0^2}{\epsilon^2\kappa^2h^2} + A^2\kappa^2\cosh^2(\kappa x) + \frac{2A\sigma_0}{\epsilon h}\cosh(\kappa x) + A^2\kappa^2\sinh^2(\kappa x) & \text{if } |x| \le L. \end{cases} \tag{80}$$

Hence, the total force is

$$F = -2\int_0^\infty \Sigma_{zz}\, dx = \frac{\sigma_0^2 L}{\epsilon\kappa^2 h^2}\left[1 - \frac{1-\exp(-2\kappa L)}{2\kappa L}\right] \tag{81}$$

and on dividing by $2L$, (26) follows.

The total charge in $x > L$ is

$$Q = -2h\epsilon\kappa^2 \int_L^\infty \overline{\phi}\, dx = -2h\epsilon\kappa B\mathrm{e}^{-\kappa L} = -\frac{2\sigma_0}{\kappa[1+\coth(\kappa L)]}. \tag{82}$$

This is the amount of charge needed to neutralize a length $\Lambda = -Q/(2\sigma_0)$ along the interface, the "lost length" [24]. Using (82) for Q, (29) follows.

Equation (26) may also be derived by contour integration (in the complex plane) of the integral (25), which is the real part of

$$I = \frac{1}{2\pi p}\int_{-\infty}^{+\infty} \frac{1-\exp(2ipz)}{z^2(1+z^2)}\, dz, \tag{83}$$

where $p = \kappa L$. We consider a closed contour $C = C_0 \cup C_\varepsilon \cup C_R$, where $C_0 = (-\infty, -\varepsilon) \cup (\varepsilon, \infty)$, C_ε is the semicircle with center at the origin and radius $\varepsilon > 0$ that lies in the upper half $\Im(z) > 0$ of the complex plane, and C_R is the semicircle with center at the origin and radius $R \gg 1$, again in the upper half $\Im(z) > 0$ of the complex plane. We take the limit $\varepsilon \to 0$ and $R \to \infty$. Denoting by I_0, I_ε and I_R the contributions to the integral from the parts of the domain C_0, C_ε and C_R and evaluating the residue from the pole at $z = i$, we find $I_0 + I_\varepsilon + I_R = (\exp(-2p) - 1)/(2p)$. Clearly, $I_R \to 0$ as $R \to \infty$ and $I_\varepsilon \to -1$ as $\varepsilon \to 0$. Thus,

$$I = 1 - \frac{1}{2p}\left[1 - \exp(-2p)\right], \tag{84}$$

and (26) follows.

References

[1] Russel, W. B., Saville, D. A., and Schowalter, W. R. (1989) *Colloidal Dispersions*. Cambridge University Press, google-Books-ID: 3shp8Kl6YoUC.

[2] Zhang, J., Luijten, E., and Granick, S. (2015) Toward Design Rules of Directional Janus Colloidal Assembly. *Annual Review of Physical Chemistry*, **66**, 581–600.

[3] Danov, K. D. (2004) Effect of Surfactants on Drop Stability and Thin Film Drainage. Starov, V. and Ivanov, I. (eds.), *Fluid Mechanics of Surfactant and Polymer Solutions*, pp. 1–38, no. 463 in International Centre for Mechanical Sciences, Springer, dOI: 10.1007/978-3-7091-2766-7_1.

[4] Derjaguin, B. and Landau, L. (1941) Theory of the Stability of Strongly Charged Lyophobic Sols and of the Adhesion of Strongly Charged Particles in Solutions of Electrolytes. *Acta Phys. Chim. URSS*, **14**, 633–662.

[5] Verwey, E. J. W. and Overbeek, J. T. G. (1999) *Theory of the Stability of Lyophobic Colloids*. Dover Publications.

[6] Bell, G. M., Levine, S., and McCartney, L. N. (1970) Approximate methods of determining the double-layer free energy of interaction between two charged colloidal spheres. *Journal of Colloid and Interface Science*, **33**, 335–359.

[7] Bhattacharjee, S. and Elimelech, M. (1997) Surface Element Integration: A Novel Technique for Evaluation of DLVO Interaction between a Particle and a Flat Plate. *Journal of Colloid and Interface Science*, **193**, 273–285.

[8] McCartney, L. N. and Levine, S. (1969) An improvement on Derjaguin's expression at small potentials for the double layer interaction energy of two spherical colloidal particles. *Journal of Colloid and Interface Science*, **30**, 345–354.

[9] Schnitzer, O. and Morozov, M. (2015) A generalized Derjaguin approximation for electrical-double-layer interactions at arbitrary separations. *The Journal of Chemical Physics*, **142**, 244102.

[10] White, L. R. (1983) On the Deryaguin approximation for the interaction of macrobodies. *Journal of Colloid and Interface Science*, **95**, 286–288.

[11] Israelachvili, J. (1987) Solvation forces and liquid structure, as probed by direct force measurements. *Acc. Chem. Res.*, **20**, 415–421.

[12] Israelachvili, J. N. (1978) Measurement of forces between surfaces immersed in electrolyte solutions. *Faraday Discussions of the Chemical Society*, **65**, 20–24.

[13] Tabor, D. and Winterton, R. H. S. (1968) Surface Forces: Direct Measurement of Normal and Retarded van der Waals Forces. *Nature*, **219**, 1120–1121.

[14] Tabor, D. (1969) Recent studies of short range forces. *Journal of Colloid and Interface Science*, **31**, 364–371.

[15] White, L. R., Israelachvili, J. N., and Ninham, B. W. (1976) Dispersion interaction of crossed mica cylinders: a reanalysis of the Israelachvili–Tabor experiments. *Journal of the Chemical Society, Faraday Transactions 1: Physical Chemistry in Condensed Phases*, **72**, 2526–2536.

[16] Todd, B. A. and Eppell, S. J. (2004) Probing the Limits of the Derjaguin Approximation with Scanning Force Microscopy. *Langmuir*, **20**, 4892–4897.

[17] Gutsche, C., Keyser, U. F., Kegler, K., Kremer, F., and Linse, P. (2007) Forces between single pairs of charged colloids in aqueous salt solutions. *Physical Review E*, **76**, 031403.

[18] Sugimoto, T., Takahashi, T., Itoh, H., Sato, S.-i., and Muramatsu, A. (1997) Direct Measurement of Interparticle Forces by the Optical Trapping Technique. *Langmuir*, **13**, 5528–5530.

[19] Israelachvili, J. N. and Ninham, B. W. (1977) International Conference on Colloids and Surfaces Intermolecular forces – the long and short of it. *Journal of Colloid and Interface Science*, **58**, 14–25.

[20] Ninham, B. W. (1999) On progress in forces since the DLVO theory. *Advances in Colloid and Interface Science*, **83**, 1–17.

[21] Bell, G. M. and Peterson, G. C. (1972) Calculation of the electric double-layer force between unlike spheres. *Journal of Colloid and Interface Science*, **41**, 542–566.

[22] Boon, N. and Roij, R. v. (2011) Charge regulation and ionic screening of patchy surfaces. *The Journal of Chemical Physics*, **134**, 054706.

[23] Ninham, B. W. and Parsegian, V. A. (1971) Electrostatic potential between surfaces bearing ionizable groups in ionic equilibrium with physiologic saline solution. *Journal of Theoretical Biology*, **31**, 405–428.

[24] Ghosal, S. and Sherwood, J. D. (2016) Repulsion Between Finite Charged Plates with Strongly Overlapped Electric Double Layers. *Langmuir*, **32**, 9445–9450.

[25] Christenson, H. K. and Claesson, P. M. (2001) Direct measurements of the force between hydrophobic surfaces in water. *Advances in Colloid and Interface Science*, **91**, 391–436.

[26] Meyer, E. E., Lin, Q., Hassenkam, T., Oroudjev, E., and Israelachvili, J. N. (2005) Origin of the long-range attraction between surfactant-coated surfaces. *Proceedings of the National Academy of Sciences of the United States of America*, **102**, 6839–6842.

[27] Perkin, S., Kampf, N., and Klein, J. (2006) Long-Range Attraction between Charge-Mosaic Surfaces across Water. *Physical Review Letters*, **96**, 038301.

[28] Kostoglou, M. and Karabelas, A. J. (1992) The effect of discrete surface charge on potential energy of repulsion between colloidal surfaces. *Journal of Colloid and Interface Science*, **151**, 534–545.

[29] Muller, V. M. and Derjaguin, B. V. (1983) Influence of the discreteness of nonlocalized charges on the interaction between the surfaces on their approach to one another. *Colloids and Surfaces*, **6**, 205–220.

[30] Richmond, P. (1975) Electrical forces between particles with discrete periodic surface charge distributions in ionic solution. *Journal of the Chemical Society, Faraday Transactions 2: Molecular and Chemical Physics*, **71**, 1154–1163.

[31] White, T. O. and Hansen, J.-P. (2002) Increased disjoining pressure between charge-modulated surfaces. *Journal of Physics: Condensed Matter*, **14**, 7649.

[32] Richmond, P. (1974) Electrical forces between particles with arbitrary fixed surface charge distributions in ionic solution. *Journal of the Chemical Society, Faraday Transactions 2: Molecular and Chemical Physics*, **70**, 1066–1073.

[33] Ben-Yaakov, D., Andelman, D., and Diamant, H. (2013) Interaction between heterogeneously charged surfaces: Surface patches and charge modulation. *Physical Review E*, **87**, 022402.

[34] Miklavic, S. J., Chan, D. Y. C., White, L. R., and Healy, T. W. (1994) Double Layer Forces between Heterogeneous Charged Surfaces. *The Journal of Physical Chemistry*, **98**, 9022–9032.

[35] Philipse, A. P., Kuipers, B. W. M., and Vrij, A. (2013) Algebraic Repulsions between Charged Planes with Strongly Overlapping Electrical Double Layers. *Langmuir*, **29**, 2859–2870.

[36] Philipse, A. and Vrij, A. (2011) The Donnan equilibrium: I. On the thermodynamic foundation of the Donnan equation of state. *Journal of Physics: Condensed Matter*, **23**, 194106.

[37] Abramowitz, M. and Stegun, I. A. (1964) *Handbook of Mathematical Functions: With Formulas, Graphs, and Mathematical Tables*. Courier Corporation, google-Books-ID: MtU8uP7XMvoC.

[38] Velegol, D. and Thwar, P. K. (2001) Analytical Model for the Effect of Surface Charge Nonuniformity on Colloidal Interactions. *Langmuir*, **17**, 7687–7693.

[39] Leote de Carvalho, R. J. F., Trizac, E., and Hansen, J.-P. (1998) Non-linear Poisson-Boltzmann theory for swollen clays. *EPL (Europhysics Letters)*, **43**, 369.

[40] Thamida, S. K. and Chang, H.-C. (2002) Nonlinear electrokinetic ejection and entrainment due to polarization at nearly insulated wedges. *Physics of Fluids*, **14**, 4315–4328.

[41] Yariv, E. (2004) Electro-osmotic flow near a surface charge discontinuity. *Journal of Fluid Mechanics*, **521**, 181–189.